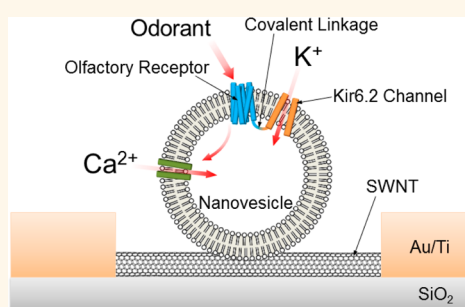


# Ion-Channel-Coupled Receptor-Based Platform for a Real-Time Measurement of G-Protein-Coupled Receptor Activities

Jong Hyun Lim,<sup>†</sup> Eun Hae Oh,<sup>‡</sup> Juhun Park,<sup>§</sup> Seunghun Hong,<sup>\*,§,⊥</sup> and Tai Hyun Park<sup>\*,†,‡,||</sup>

<sup>†</sup>School of Chemical and Biological Engineering, <sup>‡</sup>Interdisciplinary Program for Bioengineering, <sup>§</sup>Department of Physics and Astronomy, and <sup>⊥</sup>Department of Biophysics and Chemical Biology, Seoul National University, Seoul 151-744, Republic of Korea and <sup>||</sup>Advanced Institutes of Convergence Technology, Suwon, Gyeonggi-do 443-270, Republic of Korea

**ABSTRACT** A simple but efficient measurement platform based on ion-channel-coupled receptors and nanovesicles was developed for monitoring the real-time activity of G-protein-coupled receptors (GPCRs). In this work, an olfactory receptor (OR), the most common class A GPCR, was covalently fused with a Kir6.2 channel so that the GPCR action directly induced the opening of the ion channels and changes in the electrical membrane potential without complex cellular signaling processes. This strategy reduced the measurement errors caused by instability of various cellular components. In addition, rather than using whole cells, a cell-surface-derived nanovesicle was used to preserve the membrane-integrated structure of GPCRs and to exclude case-dependent cellular conditions. Another merit of using the nanovesicle is that nanovesicles can be easily combined with nanomaterial-based field-effect transistors (FETs) to build a sensitive and stable measurement platform to monitor GPCR activities with high sensitivity in real-time. Using a platform based on carbon nanotube FETs and nanovesicles carrying Kir6.2-channel-coupled ORs, we monitored the real-time response of ORs to their ligand molecules. Significantly, since this platform does not rely on rather unstable cell signaling pathways, our platform could be utilized for a rather long time period without losing its functionality. This system can be utilized extensively for simple and sensitive analysis of the activities of various GPCRs and should enable various academic and practical applications.



**KEYWORDS:** ion-channel-coupled receptor · nanovesicle · carbon nanotube · Kir6.2 · G-protein-coupled receptor

Cells continually react to their environment, and this reaction is mainly modulated by numerous membrane-integrated receptors that sense a variety of molecules outside the cells and generate cellular responses by activating signal transduction pathways. In particular, G-protein-coupled receptors (GPCRs) constitute the largest family of integral membrane proteins.<sup>1</sup> Because GPCRs play critical roles in cell responses, up to 50% of current medicinal drugs target them.<sup>2</sup> However, the analysis of their functions is quite difficult due to complicated signal transduction pathways. Cellular signal transduction generated by GPCRs requires many cellular components, such as G-proteins, secondary messengers, ion channels, and even cell organelles.<sup>3,4</sup>

The signaling pathway triggered by GPCRs can be mimicked by cell-derived nanovesicles.<sup>5</sup> Nanovesicles can be isolated from parent cells by treatment with cytochalasin B.<sup>5</sup> The nanovesicles carry membrane proteins and cytosolic components that enable the influx of Ca<sup>2+</sup> ions.<sup>6</sup> Although the detailed mechanism of Ca<sup>2+</sup> influx is unclear, previous works have demonstrated that the endogenous calcium channels in nanovesicles might be modulated by GPCR activation similar to cells.<sup>6–9</sup> The advantage of nanovesicles is that, unlike cells, the activity of the nanovesicles can be measured regardless of their viability or life cycles because they are not live cells. Also, nanovesicles can be produced in large amounts and stored for a long time,<sup>5</sup> which means that handling nanovesicles is

\* Address correspondence to seunghun@snu.ac.kr, thpark@snu.ac.kr.

Received for review November 14, 2014 and accepted January 27, 2015.

Published online January 27, 2015  
10.1021/nn506494e

© 2015 American Chemical Society

relatively easier and more efficient than handling cells. Furthermore, nanovesicles can be combined with nanomaterial-based electronic platforms by virtue of their small size. This integration allows an extremely sensitive real-time monitoring of GPCR activity.<sup>6–9</sup> Therefore, the use of nanovesicles is a good alternative to cells; however, an important issue to be solved is the stability of cellular components. The activity of all cellular components has to be stably maintained to accurately analyze the responses of GPCRs.

Ion-channel-coupled receptors can be used to solve this issue. GPCRs fused with Kir6.2, a potassium channel, directly generate an influx of positive ions, which is the final result of the original cell signaling, while bypassing complex cellular signal transduction processes.<sup>10,11</sup> The binding of ligands to GPCRs induces conformational changes in the GPCRs. The conformational change directly results in the activation of the Kir6.2 channels and consequently induces the influx of potassium ions. Thus, nanovesicles carrying ion-channel-coupled GPCRs can be used to fabricate a simple and sensitive analysis system for the measurement of subtle GPCR actions. In this work, the olfactory receptor (OR), which belongs to the largest group of class A GPCRs, was used as a representative GPCR because the function of several ORs has been clearly identified.<sup>12,13</sup>

Herein, we report a simple but powerful platform based on ion-channel-coupled receptors for the real-time measurement of GPCR activities. In this experiment, we prepared nanovesicles carrying ion-channel-coupled GPCRs and fixed them on field-effect transistor (FET) devices based on single-walled carbon nanotubes (SWNTs). In this case, the GPCR actions caused by the binding of ligand molecules directly induced the opening of Kir6.2 channels. Thus, membrane potential of nanovesicles subsequently changed without intermediate cellular processes, and this change was measured by the underlying FET device. Using this strategy, we can monitor the real-time activity of GPCRs. Significantly, since this strategy does not rely on intermediate cellular processes which might be unstable, our platform could be stored for a long time period for reliable measurements. Considering that the stability and reliability has been a major hurdle holding back the practical applications of previous nanovesicle-based devices, our strategy can be a significant breakthrough which should enable versatile academic and industrial applications such as basic research on GPCR activities, drug screening, and bioelectronic nose system development.

## RESULTS AND DISCUSSION

The olfactory system generates biological signals through cyclic adenosine monophosphate (cAMP)- and inositol 1,4,5-triphosphate (IP<sub>3</sub>)-mediated pathways.<sup>14</sup> Odorants first bind to ORs expressed on the surface of

olfactory sensory neurons in the nasal cavity. This binding event triggers activation of the  $\alpha$ -subunit of G-proteins, and secondary messengers (cAMP and IP<sub>3</sub>) are subsequently synthesized. The cyclic-nucleotide-gated (CNG) channels in the plasma membrane and calcium channels in the endoplasmic reticulum finally open, leading to an influx of Na<sup>+</sup> and Ca<sup>2+</sup> ions and an efflux of Cl<sup>-</sup> ions through chloride channels. This signaling pathway generates a depolarization on the membrane potential of neurons.<sup>15–17</sup>

Cellular systems based on human embryonic kidney (HEK)-293 cells expressing OR proteins have been utilized to analyze the signals of olfactory neurons *in vitro*.<sup>18,19</sup> HEK-293 cells do not contain CNG channels, unlike olfactory sensory neurons.<sup>20</sup> Nevertheless, HEK-293 cells can induce extracellular calcium influx through a GPCR signaling process using their endogenous calcium channels.<sup>21,22</sup> When nanovesicles were prepared from OR-expressing HEK-293 cells, the nanovesicles can also induce an increase in intracellular Ca<sup>2+</sup> ions using endogenous cellular components and ORs artificially expressed on the cell membrane.<sup>6–8</sup> The influx of calcium ions from the extracellular environment into nanovesicles has been demonstrated in previous works.<sup>6</sup> Thus, nanovesicles can be utilized as an alternative to cells. Nanovesicles are particularly suitable to apply to extremely sensitive electronic platforms based on nanomaterials, such as SWNTs and conducting polymer nanotubes.<sup>6–9,23,24</sup>

In this work, Kir6.2-channel-coupled OR (OR-Kir) was used instead of OR itself. The Kir6.2 channel, one of the inward-rectifier potassium channels, is originally coupled with sulfonylurea receptors and modulates the movement of potassium ions.<sup>25,26</sup> We covalently fused this channel at the C-terminal end of the human OR. Particularly, hOR2AG1 was used because its specific ligand, amyl butyrate, has been well-described.<sup>12,13</sup> The OR-Kir was overexpressed in HEK-293 cells, and cell-derived nanovesicles were produced using cytochalasin B. The produced nanovesicles were combined with single-walled carbon nanotube field-effect transistors (SWNT-FETs). The SWNT-FETs converted biological signals generated from the nanovesicles into highly sensitive responses that could be measured electrically (Figure 1).

The presence of OR-Kir proteins in the nanovesicles was confirmed by Western blot analysis, as shown in Figure 2a. The figure shows a band of OR-Kir proteins, which represents the presence of the OR-Kir in nanovesicles. Then, we checked whether ion influx into the nanovesicles occurred (Figure 2b). The influx of positive ions was one of the most obvious results caused by cell signal transduction. FLIPR membrane potential dye, which emits fluorescence as positive ions flow into the cells, was used.<sup>27</sup> By injecting amyl butyrate, fluorescence intensity increased in the nanovesicles

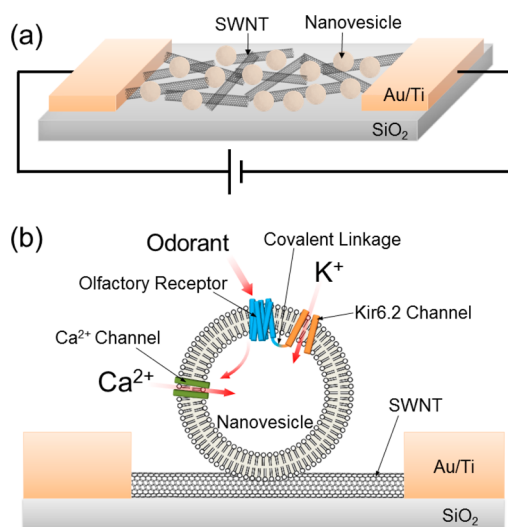


**Figure 1.** Overall schematic diagrams of the analysis system and mechanism. (a) Schematic diagram showing a nanovesicle-immobilized single-walled carbon nanotube-field effect transistor (SWNT-FET). SWNTs were randomly assembled on a SiO<sub>2</sub> substrate, and the nanovesicles were electrostatically immobilized on the SWNT channel region using poly-D-lysine. (b) Analysis mechanism of the fabricated system which consists of SWNT-FETs and nanovesicles carrying Kir6.2-channel-coupled ORs (OR-Kir). The activation of ORs induces an influx of K<sup>+</sup> ions through the Kir6.2 channels as well as an influx of Ca<sup>2+</sup> ions. Inflow of positive ions acts as a kind of gate potential; hence, the conductance on the SWNT transistor changes.

carrying OR-Kir. However, no change in fluorescence intensity was observed in nanovesicles without OR-Kir. This result clearly shows that the OR-Kir which is present on the surface of nanovesicles induced an inflow of positive ions such as K<sup>+</sup> and Ca<sup>2+</sup> ions.

Nanovesicles originated from HEK-293 cells, and the ionic composition in the nanovesicles would be similar to that of cytoplasm of cells at least in the first moment of their preparation. Therefore, the initial concentration of K<sup>+</sup> ions in the nanovesicles might be much higher than that in the extracellular medium.<sup>28</sup> However, this ionic balance could not be maintained during the storage of nanovesicles due to a deficiency of energy sources for the homeostatic maintenance. K<sup>+</sup> ions could be rapidly replaced by Na<sup>+</sup> ions in the external buffer containing 140 mM NaCl, and adding 2 mM K<sup>+</sup> in the external buffer could induce an inflow of K<sup>+</sup> ions.

The nanovesicles were immobilized on SWNT-FETs so that the SWNT-FET could monitor the signals from nanovesicles. Because the nanovesicles were derived from cells, the surface membrane of the nanovesicles had negative charges. The SWNT channels were pre-coated with poly-D-lysine (PDL) to immobilize the nanovesicles. PDL is a positively charged molecule; thus, immobilization was simply performed through a charge–charge interaction. Figure 3 shows the nanovesicles attached to the SWNT channel. SWNTs were randomly assembled on the SiO<sub>2</sub> surface, and

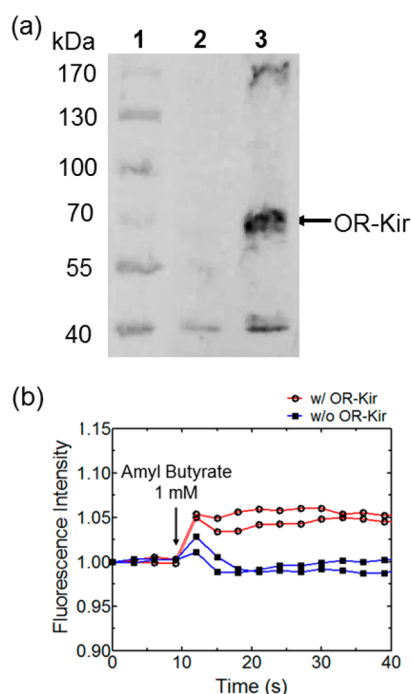


**Figure 2.** Characterization of nanovesicles carrying OR-Kir. (a) Western blot image confirming the presence of OR-Kir proteins in nanovesicles. Lanes 1, 2, and 3 indicate protein ladder, nanovesicles produced from cells without OR-Kir, and nanovesicles produced from cells with OR-Kir, respectively. (b) Real-time monitoring of an influx of positive ions into the nanovesicles. Fluorescent dye, which emits fluorescence by an influx of positive ions, was used (FLIPR membrane potential assay). Amyl butyrate (1 mM) around the nanovesicles induced ion influx into nanovesicles carrying OR-Kir.

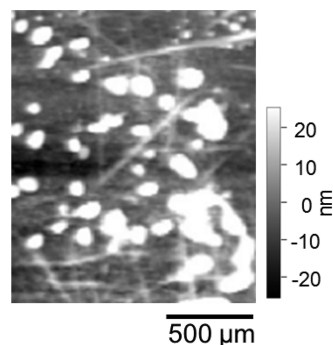


**Figure 3.** Atomic force microscopy image showing nanovesicles (bright circular spots) immobilized on the SWNT channel (bright lines). Nanovesicles were immobilized very close to randomly linked SWNTs.

the nanovesicles were attached very close to the SWNTs.

The OR-Kir present on the surface of the nanovesicles can recognize its ligand odorants. The binding event between ORs and ligands triggers direct activation of the Kir6.2 channel as well as extracellular Ca<sup>2+</sup> influx processes. As a result, positive ions flow into the nanovesicles (Figure 2b) and act as a kind of gate potential to the SWNT transistors.<sup>6</sup> Consequently,

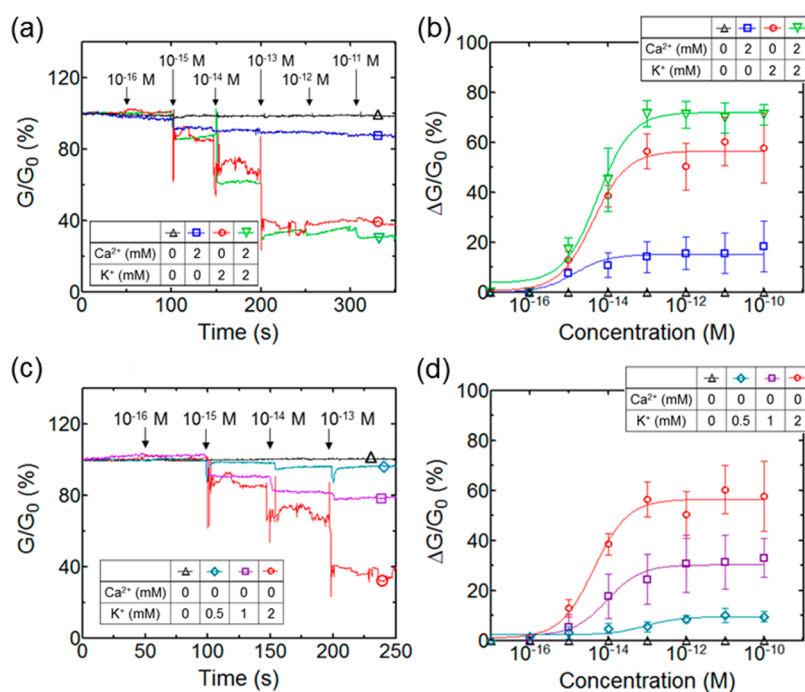


**Figure 4.** Real-time measurement of olfactory signals generated by nanovesicles carrying OR-Kir. (a) Real-time monitoring of conductance changes generated by injecting amyl butyrate. The responses were detected from  $10^{-15}$  M and saturated at  $10^{-13}$  M of amyl butyrate. (b) Dose-dependent response patterns to amyl butyrate. Each data point and error bar indicates the mean and standard deviation (SD) values, respectively ( $n = 5$ ). Conductance changes generated by potassium influx were much larger than those generated by calcium influx. (c) Real-time monitoring of conductance changes in buffer solutions with different concentrations of potassium ions. (d) Effect of external  $K^+$  concentrations on response intensity. Each data point and error bar indicates the mean and SD values, respectively ( $n = 5$ ). Note that when higher concentrations of potassium ions were in the buffer solution, greater conductance changes occurred.

conductance decreases due to the p-type semiconducting property of SWNTs.<sup>6–8,29</sup> The activity of ORs can be monitored by monitoring the change in the conductance of the SWNT transistors.

Olfactory signals from nanovesicles were measured under four different conditions to confirm the characteristics of nanovesicles carrying OR-Kir (Figure 4a,b). The first condition had no calcium or potassium ions in the buffer solution. No change in conductance by the ligands was observed when both ions were absent from the buffer solution. The second condition had only calcium ions without potassium ions, which ensured that the nanovesicles could utilize the  $Ca^{2+}$  influx processes but not the Kir6.2 channels. In contrast to the second condition, the third condition had only potassium ions without calcium ions. If there are no calcium ions in the buffer solution, only potassium ion influx is generated through the Kir6.2 channels fused with ORs. In both the second and third conditions, adding  $10^{-15}$  M (1 fM) amyl butyrate induced a prompt change in conductance. The detection limit was at  $10^{-15}$  M in both conditions; however, the response generated by the potassium influx was much higher than that generated by calcium influx. In the fourth condition, both ions were present in the buffer solution. The signal intensity was most enhanced in this condition. These results show that when the ligand was applied, a greater amount of potassium ions entered

the nanovesicles than calcium ions. The inflow of potassium ions through the Kir6.2 channels does not require cellular processes, and the large response by the Kir6.2 channel allows the sensor to efficiently discriminate specific responses from noises.

Next, the potassium concentrations in the buffer solution were changed (Figure 4c,d). As the buffer solution contained the higher concentration of potassium ions, the larger conductance changes were observed. However, the detection limit was all the same at  $10^{-15}$  M. The highest response was obtained when the buffer solution contained 2 mM potassium ions. This potassium ion concentration-dependent response indicates that Kir6.2 channels are directly modulated by the activation of ORs without any interference from other cellular components. However, when the analysis was performed with concentrations higher than 2 mM, the response was neither stable nor reproducible. Presumably, it is because the high ionic strength might influence activity and stability of nanovesicles.

Figure 4c,d shows that the signals depend on the  $K^+$  ion concentration in the buffer solution. Therefore, the recorded  $K^+$  signals are considered to be due to the  $K^+$  ion influx, which is caused by opening the Kir6.2 channels. However, we can think another possibility. In cells, Kir6.2 channels are closed by intracellular ATP, and the fused Kir6.2 is weakly opened. In nanovesicles, the inner ATP concentration may drop rapidly due to

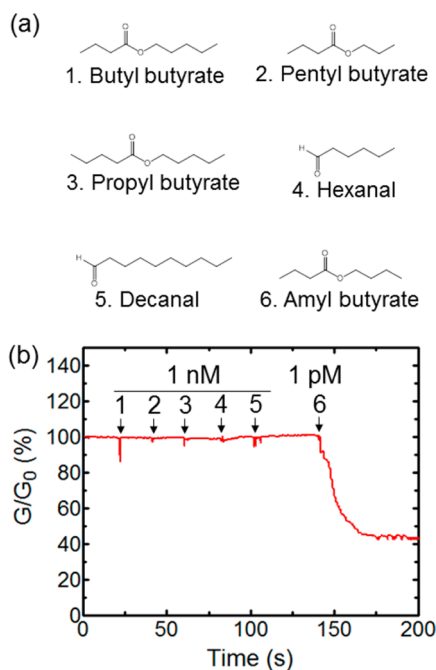


**Figure 5.** Selective response of nanovesicles carrying OR-Kir. (a) Chemical structures of amyl butyrate and its analogous compounds. Molecule names are (1) butyl butyrate, (2) pentyl valerate, (3) propyl butyrate, (4) hexanal, (5) decanal, and (6) amyl butyrate. (b) Real-time measurement of conductance changes by injecting amyl butyrate and analogous compounds. Injection of 1 pM amyl butyrate induced a decrease in conductance, whereas no changes were observed after injecting 1 nM of other compounds.

the endogenous ATPases such as the Na/K antiporters. If this is the case, the Kir6.2 channel probably opens more with time. As ion-channel-coupled receptors can be activated or inhibited by GPCR ligands,<sup>30,31</sup> we cannot exclude the possibility that the recorded  $K^+$  signals are due to closing of Kir6.2 in the presence of ligands. Further investigation is required to fully understand the sensing mechanism.

The selective response of nanovesicles carrying OR-Kir was also examined. In general, some ORs have excellent selectivity capable of discriminating their specific ligands.<sup>29,32</sup> hOR2AG1, which was used in this study, interacts only with amyl butyrate, its specific ligand.<sup>6</sup> We examined whether the selectivity of the receptor was maintained even after the Kir6.2 channel was covalently coupled with the receptor. As shown in Figure 5a, the chemical structures of the compounds used in this experiment were very similar to that of amyl butyrate. Moreover, the concentration of analogous compounds used to stimulate the receptor was much higher than that of amyl butyrate. Nevertheless, the OR-Kir precisely discriminated amyl butyrate (Figure 5b) among other analogous odorants. This indicates that the selectivity of hOR2AG1 was retained despite the fusion with Kir6.2 channels.

$Ca^{2+}$  influx processes require various cellular components, which should be stably maintained for an accurate analysis. The activity of conventional

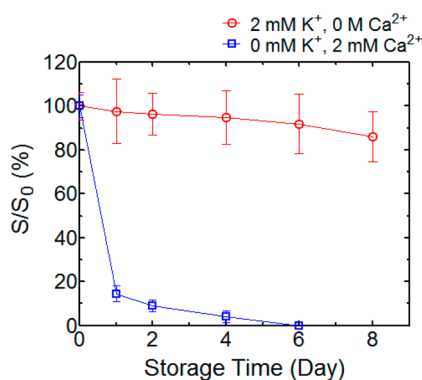


**Figure 6.** Stability of nanovesicles carrying OR-Kir in a nonfrozen state. The nanovesicle-immobilized SWNT-FETs were stored for a different number of days at 4 °C. More than 85% of sensor activity was maintained for up to 8 days when Kir6.2-channel-mediated signaling was used. However, ATP-mediated calcium signaling was extinguished within 4 days. Amyl butyrate concentration used in this experiment was  $10^{-13}$  M. Each data point and error bar indicates the mean and SD values, respectively ( $n = 3$ ).

nanovesicles using  $Ca^{2+}$  influx depends on the activities of these cellular components and consequently depends on the handling and storage conditions of nanovesicles. This might be one of the critical drawbacks of nanovesicles using  $Ca^{2+}$  influx. However, the Kir6.2 channel is physically opened by a conformational change in the OR without the involvement of other cellular components.<sup>10</sup> Therefore, nanovesicles carrying OR-Kir can stably generate olfactory signals regardless of storage conditions that may cause a destabilization of intracellular signaling components.

To test the stability of our platform, nanovesicle-immobilized SWNT-FETs were stored at 4 °C for several days, and the remaining activity in nanovesicles after storage was measured (Figure 6). Significantly, more than 85% of Kir6.2-channel-mediated signaling activity was maintained for up to 8 days of storage, whereas the signals generated by  $Ca^{2+}$  influx were completely extinguished within 4 days. This result clearly shows that the stability of our nanovesicle-based devices was remarkably improved by coupling the Kir6.2 channels with the ORs.

Nanovesicles have various advantages as cell-mimicking materials. They can generate GPCR signals with a mechanism similar to that of a cell. Storage of nanovesicles is much easier than cells, and the nanovesicles are suitable to build nanomaterial-based FET platforms. The integration of nanovesicles and FET platforms facilitates the sensitive measurement of GPCR activities.<sup>9</sup> However, conventional nanovesicles without Kir6.2 channels rely on multiple steps of signal transduction for converting GPCR activities to measurable electrical signals. Therefore, it is critical to maintain the complex signal transduction processes in the conventional nanovesicles. On the other hand, in the nanovesicles carrying ion-channel-coupled receptors,

GPCR activities can be directly transduced to the measurable signals without relying on the complex signal transduction processes. Thus, the long-term stability and reliability can be dramatically enhanced.

## CONCLUSION

In this work, Kir6.2-channel-coupled receptors were expressed in HEK-293 cells, and nanovesicles were produced from the cells. The receptors in the surface of nanovesicles recognized their ligand molecules and directly activated the fused Kir6.2 channels without the aid of other cellular components. Because this system does not use the cellular signaling processes, the action of GPCRs could be analyzed without the influence of other signaling components. The use of cell-derived nanovesicles had the merit of guaranteeing a

proper structure of integral membrane proteins as well as being produced in large quantities and being conveniently stored for a long time. The nanovesicles were conjugated with SWNT-FET platforms to effectively monitor the activity of GPCRs. The subtle change in the structure of GPCRs induced the influx of potassium ions through the Kir6.2 channels, and this influx was transduced into electronic signals with high sensitivity by SWNT-FETs. Consequently, the system, which comprised Kir6.2-channel-coupled receptors, nanovesicles, and FET platforms, facilitated the simple and sensitive analysis of the GPCR responses to ligand molecules. This system should open up various academic and industrial applications such as drug screening and bioelectronic nose development.<sup>7–9</sup>

## MATERIALS AND METHODS

**Gene Cloning and Transfection.** OR genes do not contain intron. The hOR2AG1, one of the human OR genes, was amplified by polymerase chain reaction from the human genomic DNA (Novagen, Madison, WI, USA). The Kir6.2 channel was fused to the C-terminal of hOR2AG1. Twenty-five N-terminal amino acid sequences in the Kir6.2 channel were excluded to achieve an effective conformational change in the channel.<sup>10,11</sup> The *Flag-tag* and *rho-tag* were fused at the N-terminus of hOR2AG1 to assist with membrane localization and immunoblot assaying of the receptor, respectively. The Kir6.2-channel-fused hOR2AG1 was inserted into pcDNA3 vector (Invitrogen, Carlsbad, CA, USA). HEK-293 cells were cultured in Dulbecco's modified Eagle's medium (DMEM; WelGENE, Daegu, South Korea) with 10% fetal bovine serum (Gibco, Grand Island, NY, USA) and 1% penicillin–streptomycin (Gibco) at 37 °C in a humidified 5% CO<sub>2</sub> incubator. Transfection was conducted using a Neon Transfection System (Invitrogen). The cells were harvested and resuspended at a density of  $1.5 \times 10^7$  cells mL<sup>-1</sup>. Then, 100  $\mu$ L of cell solution was mixed with 5  $\mu$ g of pcDNA3 plasmids containing Kir6.2-fused OR genes. After being mixed, electric pulses (1100 V, 3  $\times$  10 ms) were applied to the cells. The cells were cultured for 48 h in fresh medium.

**Production of Nanovesicles.** Nanovesicles were produced from HEK-293 cells by incubating the cells in DMEM containing 10  $\mu$ g mL<sup>-1</sup> cytochalasin B (Sigma, St Louis, MO, USA) at 37 °C for 25 min in a shaking incubator.<sup>9</sup> The cells were separated by centrifugation at 500g for 10 min. The nanovesicles were finally isolated by centrifugation at 15 000g for 30 min. The nanovesicles were resuspended in Dulbecco's phosphate-buffered saline (dPBS; Gibco) with 1000 ng mL<sup>-1</sup> total protein density. The nanovesicles were stored at –80 °C.

**Immunoblot Analysis.** The nanovesicles were lysed by sonication (2 s on/off, 5 min). The membrane fraction of the nanovesicle lysates was separated by centrifugation at 15 000g for 30 min. The prepared sample was separated by sodium dodecyl sulfate polyacrylamide gel electrophoresis and transferred to a polyvinylidene difluoride membrane (PVDF; Bio-Rad, Hercules, CA, USA) over a period of 60 min under 0.15 A of constant current. The PVDF membranes were blocked with a PBS solution containing 5 wt % skim milk and 0.1 v% Tween-20 for 2 h. The membranes were then incubated overnight at 4 °C in PBS-T (0.1% Tween-20 in PBS) solution containing 1:1000-diluted anti-flag antibody (Cell Signaling, Beverly, MA, USA). The membrane was incubated in PBS-T solution containing horseradish peroxidase (HRP)-conjugated anti-rabbit antibody (Amersham-Pharmacia Biotech, Cambridge, UK) for 2 h at room temperature. HRP luminescence was measured using an enhanced chemiluminescence HRP substrate (SuperSignal West Dura

Extended Duration Substrate; Thermo Scientific, Waltham, MA, USA). The Western blot image was taken with the G:BOX Chemi XL system (Syngene, Cambridge, UK).

**Preparation of Buffer and Odorant Solutions.** Buffer solution (10 mM HEPES, 140 mM NaCl, 2 mM KCl, and 2 mM CaCl<sub>2</sub>, pH 7.4) was prepared. Odorant stock solutions (1 M) (amyl butyrate, butyl butyrate, pentyl butyrate, propyl butyrate, hexanal, and decanal; all from Sigma) were prepared using dimethyl sulfoxide (Sigma). Also, 1 M odorant stocks were serially diluted with the prepared buffer solution. The diluted odorants were stored at 4 °C for subsequent experiments.

**FLIPR Membrane Potential Assay.** Nanovesicles were immobilized on 96-well plates (Nunc, Roskilde, Denmark) precoated with 0.1 mg mL<sup>-1</sup> PDL by incubating at 4 °C for 2 h. After the incubation, the buffer solution was replaced with 90  $\mu$ L of fresh buffer solution (dPBS), and 90  $\mu$ L of the loading buffer included in the FLIPR membrane potential assay kit (Molecular Devices, Sunnyvale, CA, USA) was added (totally 180  $\mu$ L of buffer solution). The nanovesicles were incubated at 37 °C for 30 min. For the assay, 20  $\mu$ L of the odorant sample (10 mM) was injected to the wells using the microinjection system of GENios Pro (Tecan, Mannedorf, Germany). The odorant samples were finally diluted to 1:10 during the injection process, and final odorant concentration around the nanovesicles was 1 mM. Fluorescence emitted by excitation at 535 nm was measured at 590 nm using GENios Pro. Odorant stock (10 mM) was warmed to 37 °C for the stably dispersed phase of hydrophobic odorant. Odorant injection steps were quickly performed to avoid phase separation in the microinjector, and the injection speed was optimized at 70  $\mu$ L s<sup>-1</sup> for the effective mixing between odorant and buffer solution.

**Fabrication of Nanovesicle-Immobilized SWNT-FETs.** SWNT-FETs were fabricated by a conventional photolithography technique.<sup>33</sup> Methyl-terminated octadecyltrichlorosilane (OTS) was first patterned on a silicon substrate with a 100 nm oxide layer using the photolithography method. The OTS-patterned substrate was dipped into SWNT suspensions (0.01 mg mL<sup>-1</sup> in dichlorobenzene) for approximately 10 s. During the dipping process, SWNTs self-assembled onto the bare SiO<sub>2</sub> region. Ti (10 nm)/Au (30 nm) electrodes were deposited by photolithography and thermal evaporation techniques. The electrodes were finally passivated with an insulating photoresist to block a direct contact with the solutions. The distance between the source–drain electrodes was 15  $\mu$ m. A PDL solution (0.1 mg mL<sup>-1</sup>) was placed on the SWNT channel area for 2 h to immobilize the nanovesicles. After the channel was washed with deionized water, 1  $\mu$ L of nanovesicle solution was added to the PDL-coated SWNT channel and incubated for 2 h. During the incubation, the nanovesicles were immobilized on the PDL-coated area by a charge–charge interaction.

**Characterization of Nanovesicle Immobilization.** The immobilization of nanovesicles was confirmed using atomic force microscopy (AFM). The nanovesicles immobilized on the SWNT-FETs were fixed by treatment with 4% paraformaldehyde for 20 min at room temperature. The fixed nanovesicles were washed with deionized water, and the sample was dehydrated with ethanol. The sample was gently dried under N<sub>2</sub> gas, and the dried sample was used for AFM imaging. AFM imaging was performed under ambient conditions using an AFM system (MFP-3D; Asylum Research, Goleta, CA, USA) in intermittent mode.

**Measurement of Olfactory Signals.** Olfactory signals were measured using a Keithley 2636A sourcemeter (Keithley, Cleveland, OH, USA) and a probe station (MS Tech, Hwaseong, South Korea). A 0.1 V direct current was applied to the source–drain electrodes, and the gate voltage was grounded. Next, 49.5  $\mu$ L of buffer solution was placed on the SWNT-FETs. Then, 0.5  $\mu$ L of odorant solution was added, and the change in the source–drain currents was measured.

**Conflict of Interest:** The authors declare no competing financial interest.

**Acknowledgment.** This study was supported by the National Research Foundation of Korea (NRF) grant funded by the Ministry of Science, ICT, & Future Planning. T.H.P. appreciates support from the NRF grants (Nos. 2014039771 and 2014053108). S.H. acknowledges the support from the BioNano Health-Guard Research Center (H-GUARD 2013M3A6B2078961) and the funding programs by the Ministry of Science, ICT & Future Planning (Nos. 2014004023 and 2014M3A7B4051591).

## REFERENCES AND NOTES

- Cherezov, V.; Rosenbaum, D. M.; Hanson, M. A.; Rasmussen, S. G. F.; Thian, F. S.; Kobilka, T. S.; Choi, H.-J.; Kuhn, P.; Weis, W. I.; Kobilka, B. K.; Stevens, R. C. High-Resolution Crystal Structure of an Engineered Human  $\beta$ 2-Adrenergic G Protein-Coupled Receptor. *Science* **2007**, *318*, 1258–1265.
- Overington, J. P.; Al-Lazikani, B.; Hopkins, A. L. How Many Drug Targets Are There? *Nat. Rev. Drug Discovery* **2006**, *5*, 993–996.
- Marinissen, M. J.; Gutkind, J. S. G-Protein-Coupled Receptors and Signaling Networks: Emerging Paradigms. *Trends Pharmacol. Sci.* **2001**, *22*, 368–376.
- Ko, H. J.; Park, T. H. Dual Signal Transduction Mediated by a Single Type of Olfactory Receptor Expressed in a Heterologous System. *Biol. Chem.* **2006**, *387*, 59.
- Pick, H.; Schmid, E. L.; Tairi, A.-P.; Ilegems, E.; Hovius, R.; Vogel, H. Investigating Cellular Signaling Reactions in Single Attoliter Vesicles. *J. Am. Chem. Soc.* **2005**, *127*, 2908–2912.
- Jin, H. J.; Lee, S. H.; Kim, T. H.; Park, J.; Song, H. S.; Park, T. H.; Hong, S. Nanovesicle-Based Bioelectronic Nose Platform Mimicking Human Olfactory Signal Transduction. *Biosens. Bioelectron.* **2012**, *35*, 335–341.
- Park, S. J.; Kwon, O. S.; Lee, S. H.; Song, H. S.; Park, T. H.; Jang, J. Ultrasensitive Flexible Graphene Based Field-Effect Transistor (FET)-Type Bioelectronic Nose. *Nano Lett.* **2012**, *12*, 5082–5090.
- Lim, J. H.; Park, J.; Oh, E. H.; Ko, H. J.; Hong, S.; Park, T. H. Nanovesicle-Based Bioelectronic Nose for the Diagnosis of Lung Cancer from Human Blood. *Adv. Healthcare Mater.* **2014**, *3*, 360–366.
- Park, S. J.; Song, H. S.; Kwon, O. S.; Chung, J. H.; Lee, S. H.; An, J. H.; Ahn, S. R.; Lee, J. E.; Yoon, H.; Park, T. H.; Jang, J. Human Dopamine Receptor Nanovesicles for Gate-Potential Modulators in High-Performance Field-Effect Transistor Biosensors. *Sci. Rep.* **2014**, *4*, 4342.
- Moreau, C. J.; Dupuis, J. P.; Revilloud, J.; Arumugam, K.; Vivaudou, M. Coupling Ion Channels to Receptors for Biomolecule Sensing. *Nat. Nanotechnol.* **2008**, *3*, 620–625.
- Caro, L. N.; Moreau, C. J.; Revilloud, J.; Vivaudou, M.  $\beta$ 2-Adrenergic Ion-Channel Coupled Receptors as Conformational Motion Detectors. *PLoS One* **2011**, *6*, e18226.
- Neuhaus, E. M.; Mashukova, A.; Zhang, W.; Barbour, J.; Hatt, H. A Specific Heat Shock Protein Enhances the Expression of Mammalian Olfactory Receptor Proteins. *Chem. Senses* **2006**, *31*, 445–452.
- Gelis, L.; Wolf, S.; Hatt, H.; Neuhaus, E. M.; Gerwert, K. Prediction of a Ligand-Binding Niche within a Human Olfactory Receptor by Combining Site-Directed Mutagenesis with Dynamic Homology Modeling. *Angew. Chem., Int. Ed.* **2012**, *51*, 1274–1278.
- Firestein, S. How the Olfactory System Makes Sense of Scents. *Nature* **2001**, *413*, 211–218.
- Lee, S. H.; Jun, S. B.; Ko, H. J.; Kim, S. J.; Park, T. H. Cell-Based Olfactory Biosensor Using Microfabricated Planar Electrode. *Biosens. Bioelectron.* **2009**, *24*, 2659–2664.
- Lee, S. H.; Jeong, S. H.; Jun, S. B.; Kim, S. J.; Park, T. H. Enhancement of Cellular Olfactory Signal by Electrical Stimulation. *Electrophoresis* **2009**, *30*, 3283–3288.
- Lee, J. Y.; Ko, H. J.; Lee, S. H.; Park, T. H. Cell-Based Measurement of Odorant Molecules Using Surface Plasmon Resonance. *Enzyme Microb. Technol.* **2006**, *39*, 375–380.
- Wetzel, C. H.; Oles, M.; Wellerdieck, C.; Kuczkowiak, M.; Gisselmann, G.; Hatt, H. Specificity and Sensitivity of a Human Olfactory Receptor Functionally Expressed in Human Embryonic Kidney 293 Cells and *Xenopus laevis* Oocytes. *J. Neurosci.* **1999**, *19*, 7426–7433.
- Katada, S.; Nakagawa, T.; Kataoka, H.; Touhara, K. Odorant Response Assays for a Heterologously Expressed Olfactory Receptor. *Biochem. Biophys. Res. Commun.* **2003**, *305*, 964–969.
- Sato, K.; Pellegrino, M.; Nakagawa, T.; Nakagawa, T.; Vosshall, L. B.; Touhara, K. Insect Olfactory Receptors Are Heteromeric Ligand-Gated Ion Channels. *Nature* **2008**, *452*, 1002–1006.
- Pindon, A.; van Hecke, G.; van Gompel, P.; Lesage, A. S.; Leysen, J. E.; Jurzak, M. Differences in Signal Transduction of Two 5-HT<sub>4</sub> Receptor Splice Variants: Compound Specificity and Dual Coupling with G $\alpha$ s- and G $\alpha$ i/o-Proteins. *Mol. Pharmacol.* **2002**, *61*, 85–96.
- Lee, S. H.; Ko, H. J.; Park, T. H. Real-Time Monitoring of Odorant-Induced Cellular Reactions Using Surface Plasmon Resonance. *Biosens. Bioelectron.* **2009**, *25*, 55–60.
- Oh, E. H.; Song, H. S.; Park, T. H. Recent Advances in Electronic and Bioelectronic Noses and Their Biomedical Applications. *Enzyme Microb. Technol.* **2011**, *48*, 427–437.
- Lee, S. H.; Park, T. H. Recent Advances in the Development of Bioelectronic Nose. *Biotechnol. Bioprocess E* **2010**, *15*, 22–29.
- Isomoto, S.; Kondo, C.; Yamada, M.; Matsumoto, S.; Higashiguchi, O.; Horio, Y.; Matsuzawa, Y.; Kurachi, Y. A Novel Sulfonylurea Receptor Forms with BIR (Kir6.2) a Smooth Muscle Type ATP-Sensitive K<sup>+</sup> Channel. *J. Biol. Chem.* **1996**, *271*, 24321–24324.
- Inagaki, N.; Gonoi, T.; Iv, J. P. C.; Wang, C.-Z.; Aguilar-Bryan, L.; Bryan, J.; Seino, S. A Family of Sulfonylurea Receptors Determines the Pharmacological Properties of ATP-Sensitive K<sup>+</sup> Channels. *Neuron* **1996**, *16*, 1011–1017.
- Whiteaker, K. L.; Gopalakrishnan, S. M.; Groebe, D.; Shieh, C.-C.; Warrior, U.; Burns, D. J.; Coghlan, M. J.; Scott, V. E.; Gopalakrishnani, M. Validation of FLIPR Membrane Potential Dye for High Throughput Screening of Potassium Channel Modulators. *J. Biomol. Screen.* **2001**, *6*, 305–312.
- Zhu, G.; Zhang, Y.; Xu, H.; Jiang, C. Identification of Endogenous Outward Currents in the Human Embryonic Kidney (HEK 293) Cell Line. *J. Neurosci. Methods* **1998**, *81*, 73–83.
- Kim, T. H.; Lee, S. H.; Lee, J.; Song, H. S.; Oh, E. H.; Park, T. H.; Hong, S. Single-Carbon-Atomic-Resolution Detection of Odorant Molecules Using a Human Olfactory Receptor-Based Bioelectronic Nose. *Adv. Mater.* **2009**, *21*, 91–94.
- Niescierowicz, K.; Caro, L.; Cherezov, V.; Vivaudou, M.; Moreau, C. J. Functional Assay for T4 Lysozyme-Engineered G Protein-Coupled Receptors with an Ion Channel Reporter. *Structure* **2014**, *22*, 149–155.
- Caro, L. N.; Moreau, C. J.; Estrada-Mondragón, A.; Ernst, O. P.; Vivaudou, M. Engineering of an Artificial Light-Modulated Potassium Channel. *PLoS One* **2012**, *7*, e43766.

32. Yoon, H.; Lee, S. H.; Kwon, O. S.; Song, H. S.; Oh, E. H.; Park, T. H.; Jang, J. Polypyrrole Nanotubes Conjugated with Human Olfactory Receptors: High-Performance Transducers for FET-Type Bioelectronic Noses. *Angew. Chem., Int. Ed.* **2009**, *48*, 2755–2758.
33. Lee, M.; Im, J.; Lee, B. Y.; Myung, S.; Kang, J.; Huang, L.; Kwon, Y. K.; Hong, S. Linker-Free Directed Assembly of High-Performance Integrated Devices Based on Nanotubes and Nanowires. *Nat. Nanotechnol.* **2006**, *1*, 66–71.